

Experimental Performance of a Crossed-Field Plasma Accelerator

V. H. BLACKMAN* AND R. J. SUNDERLAND†

MHD Research, Inc., Newport Beach, Calif.

A study has been made of the thrust developed by a steady, crossed-field accelerator as a function of various operating parameters, the lifetime of the components for different accelerator geometries, and the behavior of the working fluid. A major portion of the experimental effort was directed toward the solution of material erosion problems. A satisfactory arrangement has been devised which enables tests to be conducted with little erosion of the accelerator components at power levels up to 60 kw with mass flow rates as low as 0.3 g/sec of argon. Experiments were performed with both confined and open duct accelerators. A confined duct was operated with several gases and the relative merits of each of these gases for crossed-field accelerator application are discussed. Empirical relationships for the open duct accelerator have been obtained which describe the thrust as a function of the field parameters and the mass flow rate of the expellant. With the open duct geometry, thrusts of the order of 1 lb have been achieved with argon at specific impulses greater than 1000 sec.

I. Introduction

THE results of the past year of experimental work concerning steady, crossed-field ($j \times B$) accelerators are presented. This work was a continuation of a program that already has been reported.¹ The objective has been to study the feasibility of steady, crossed-field accelerators for obtaining high gas velocity at reasonable efficiency. The determination of feasibility has entailed the study of 1) the thrust developed by an accelerator as a function of various parameters, 2) the lifetime of various components for different accelerator geometries, and 3) fluid behavior, including nonequilibrium electron conduction and deflection of the flow by Hall forces.

Measurements of thrust were made indirectly with a jet deflection technique using a thrust disk connected to a strain gage through a movable diaphragm. The thrust determination, along with the measured mass flow rate, enabled the velocity to be determined as a function of the total input power. Power levels up to 60 kw were used in the crossed-field accelerator section at mass flows as low as 0.3 g/sec.

A major effort was directed toward solving material problems, and some degree of success was achieved. The problems were essentially of two types: those associated with electrodes, including the maintenance of stable arcs, and those associated with insulator erosion. The erosion occurred principally at the downstream edge of the electrodes. This seems to be due primarily to the blowing effect of the gas flow on the arc added to the $j \times B$ force on the arc column. A satisfactory arrangement was devised which enabled high-power short time duration tests to be conducted in argon with little erosion of the accelerator components.

More subtle problems arose due to the behavior of electric currents in a gas in the presence of a magnetic field. One effect of primary importance is the increase in electron temperature (and density) in a partially ionized gas once a certain critical value of the electric field E is exceeded. A useful relation that may be used to calculate such a critical field threshold is²

$$(E/P)_{\text{critical}} > 6.6(Q_{ei}/q)(M_e/M)^{1/2}$$

Presented at the ARS 17th Annual Meeting and Space Flight Exposition, Los Angeles, Calif., November 13-18, 1962; revision received June 11, 1963. The research described herein has been performed on a subcontract from The Marquardt Corporation under NASA Contract NAS 5-1120. The authors would like to acknowledge the considerable assistance in this work which was given by Calvin Snyder and Max Minnemeier in the careful operation of the experiment and compilation of data.

* Technical Director. Member AIAA.

† Senior Research Scientist. Member AIAA.

where

p = gas pressure, nts/m²

Q_{ei} = total electron collision cross section, m² (elastic plus inelastic)

m_e = mass of electron, g

M = mass of heavy particles, g

q = electronic charge, coul

At pressures of approximately 10^{-2} atmospheres and $Q_{ei} = 10^{-16}$ cm² (e.g., argon), E critical is of the order of 10 mv/cm or less. Operation of the accelerator arcs with argon, however, requires field strengths of the order of 20 v/cm which leads to considerable electron heating, an increase in electron density (breakdown), and hence a resultant increase in conductivity. Thus, the operating characteristics of the discharge in the accelerator are almost independent of the conductivity of the gas upstream of the electrode region. In fact, the accelerator has been operated with gas flow through the plasmajet but without striking the plasmajet arc (i.e., with cold gas flowing through the de Laval nozzle). Acceleration was obtained in the crossed-field region with ionization supplied by cross arcs only. The voltage-current relationship is dominated by nonequilibrium effects due to the impressed electric fields.^{3, 4}

In the accelerator, an electric discharge is struck between electrodes transverse to a supersonic flow of gas. A magnetic field, oriented so that the "motor force" is in the proper direction to accelerate the gas, is applied to the discharge. If all of the current is carried in the region of the field (rather than blown downstream of the field), then the increase in the jet thrust F , neglecting viscous losses is

$$\begin{aligned} F &= jBAL = (I/A)BAL \\ &= BIL \end{aligned}$$

Thus, the increase in thrust is given by the product of the current flowing I , the magnetic induction B , and the separation of the electrodes L . Such a simple relation, while not expected to be highly accurate, serves to indicate the increase in thrust attainable in a crossed-field device.

II. Experimental Studies

A. Description of the Facility

Two basically different types of accelerator test sections were used. The first of these was a confined jet accelerator in which the cross-sectional area of the jet issuing from a de Laval nozzle remained approximately constant as it passed through the electrode region. An open jet accelerator, in

which the jet boundary was essentially free, was also constructed and operated in much the same mode as reported by Demetriades.⁵ In essence, the confined jet accelerator was dominated by large viscous losses that made it impossible to obtain high jet velocities. The open jet accelerator exhibited a strong Hall deflection even when powered with four independent cross arcs.

The tests, with both the confined jet and open jet, were conducted with a multiple electrode structure. Because of the gas and magnetic blowing effects on an arc, the discharge attaches in a small region at the downstream edge of any electrode structure having an extended length parallel to the streaming direction. Consequently, a considerable portion of a long electrode serves no useful purpose and can be replaced effectively by a single "point" electrode. In practice, the "point" area is determined by heat-dissipation considerations. Thus, a strip electrode can be replaced advantageously with several individually powered electrodes. In addition, the individual electrodes can be staggered and biased to eliminate the axial potentials that cause current flows resulting in unwanted beam deflections.

Because of the physical limitations in the accelerator, four electrode pairs distributed along the channel was the most satisfactory arrangement. It also allowed the use of a set of four special power supplies, one to power each arc independent of the others. The V - I characteristic of these units had a sharp enough "droop" to result in very stable arc operation in the accelerator. Three separate open-circuit voltage ranges were available from each supply, 115, 230, and 460 v.

The electrode material used was limited to graphite and tungsten. The graphite eroded appreciably at arc power levels above 5 kw and so proved unsatisfactory. The erosion appeared to occur both as normal sublimation and also as spalling of visible size particles.

Tungsten was used with much greater success. Early tests were performed with $\frac{1}{4}$ -in.-diam uncooled tungsten rods. The anode, which absorbs more power than the cathode in an arc, melted on the tip at fairly low input power levels. Modified electrodes were then made out of $\frac{1}{2}$ -in.-diam tungsten with provisions for water cooling in much the same manner as the cathode is cooled in a conventional plasmajet. With this arrangement the electrodes could be operated at approximately 10 kw in each arc without electrode erosion or even excessive melting. When the power in a particular arc exceeded 10 kw, melting of the anode tips began to appear and was more or less serious depending on the electrode shape and how well it was cooled.

Experiments with a confined, constant area jet and with electrode structures flush with the ceramic insulation led to

rapid and intolerable erosion of the ceramic at the trailing edge of the electrode. Therefore, attempts were made to hold the arc attachment point near the middle of the electrode by means of steps in the electrode. The step then should give the arc a stagnant region in which to attach. This approach relieved the erosion problem somewhat, but the erosion was still far too severe for long duration tests (e.g., >1 min).

In order to avoid the difficulties just mentioned, an apparatus was constructed to run tests on an open jet. The chamber was brass, essentially cylindrical, with a diameter of approximately 8 in. Circular holes in the sidewalls allowed the insertion of water-cooled magnet pole faces into the chamber. The pole faces were sealed by means of double O rings. In the direction transverse to the magnetic lines, four electrode pairs could be inserted with appropriate ceramic blocks for insulation. Thus the jet was in a partially confined condition in which the area was restricted greatly from the 8-in.-i.d. chamber. A window was provided which allowed visual observation of the arc region over the top of one of the magnet pole faces. The chamber was bolted directly to a thrust stand so that the jet impinged on a thrust disk for determination of the jet momentum. The maximum attainable magnetic field was of the order of 4-5 kgauss depending on pole face separation and shape.

The insulators surrounding the electrodes were of boron nitride, which was selected as the best material to use on many counts, including availability, machinability, and erosion resistance at high thermal loads. The boron nitride itself is kept $\frac{1}{2}$ in. to 1 in. back from the tip of the electrode; in order to eliminate spalling the BN is baked to remove absorbed water. The most satisfactory operation of the accelerator has been achieved with the arrangement of electrodes shown in Fig. 1.

In the open jet accelerator there was some problem with arcing to the magnet pole faces instead of through the jet, therefore, it was necessary to insulate the metal faces. This was accomplished by fastening quartz plates to the pole face with a graphite based cement. The thermal loads on the quartz were low enough so that with a separation between quartz faces of only three-quarters of an inch, the same as the exit diameter of the jet at the nozzle, there was little or no erosion of the quartz. Thus, it is concluded that the only serious materials problem in accelerator operation is at the trailing edge of the electrodes and the anode tip. In order to analyze the operation of the accelerator, it was necessary to measure and record (continuously wherever possible) a number of different parameters.

The gas mass flow rate \dot{m} was metered and measured by means of a Fisher Porter float-type flowmeter with full scale accuracy of $\pm 3\%$. At the scale level for the lowest mass flow rate, an inaccuracy of $\pm 10\%$ in the values of \dot{m} was present. Since this quantity was set and held fixed for a run and since it was very stable once set, the value of \dot{m} was not recorded continuously. The voltage and current levels in the accelerator arcs were recorded continuously. Currents were measured by use of conventional 50 mv shunts that could be changed to suit the particular current level. Voltages were taken directly across the electrodes. Since for most tests there were four separate electrode pairs, this meant eight separate quantities had to be recorded continuously. Two methods of recording were used. First, the output across one of the current shunts, usually for electrode number two, was put directly on a 50-mv galvanometer that recorded on a Consolidated Electrodynamics Corporation recorder. Thus, the current from one electrode pair was on the recorder tape. The outputs from the voltage and current channels were displayed on eight meters mounted on a suitable panel. When continuous data were required, the panel was photographed with a motion picture camera. In order to synchronize the film time with the time base on the recorder tape, provision was made to apply time blips

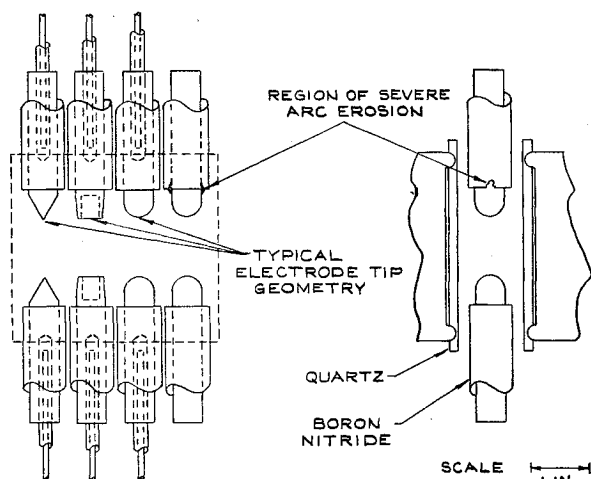


Fig. 1 General arrangement of tungsten electrodes; the types of geometries are indicated.

to the recorder tape at the same time the event was recorded on the film. The magnet current (field) also was recorded continuously on the recorder tape and displayed on a meter so that it could be photographed with other meters.

The technique used to determine thrust consisted of placing a disk at the end of the accelerator to deflect the gas flow by 90° and then determining the force exerted on the disk by a suitable coupling to an external transducer. A drawing of the thrust measuring system is shown in Fig. 2.

Few mechanical problems were encountered in the operation of the thrust system. The output of the transducer was recorded on the Consolidated Electrodynamic Corporation recorder tape so that a continuous record of the thrust was obtained. The system was calibrated by applying a force directly to the center of the thrust disk by means of gram weights and a balance arrangement. The value of the force applied could be resolved on the tape to better than 5 g-wt over a wide range of force. The means by which the force is transferred from the inside to the outside of the vacuum system is of some interest. Referring to Fig. 2, the rod supporting the thrust disk terminates at the center of a circular piece of beryllium copper, which is supported around the periphery. The beryllium copper is machined in the shape indicated in the figure to a minimum thickness of approximately 0.06 in. Any force exerted transverse to the rod, e.g., to the face of the disk, will be transferred to the outside by flexure of the disk. The strain transducer then can be mounted outside of the vacuum vessel as shown.

The major problems with the thrust system included erosion of the disk at very high input power levels and interpretation of the measured force in terms of the true jet thrust. In addition to disk erosion at high power level, there were indications that at certain operating pressures the last electrode pair would short to the graphite thrust disk. Although the disk is grounded while the power supply is floating, breakdown at low pressure could allow arcing to the disk. In order to eliminate the arcing to the graphite, magnesium oxide disks were fastened to the graphite by means of a high-temperature graphite-based cement. The magnesia eliminated the arcing problem to the thrust disk and at the same time was quite satisfactory from an erosion standpoint up to power levels of 60 kw for operation of several minutes duration.

The second problem, namely interpretation, is not as simple to solve. In order to check the relationship between the measured force and the thrust of the jet, a series of measurements using a plasmajet-de Laval nozzle arrangement were made. The force on the thrust disk exerted by the jet was compared to the calculated value using the relation

$$F = \dot{m}v = \dot{m} \left[2 \left(\frac{M^2}{M^2 + [2/(\gamma - 1)]} \right) h_0 \right]^{1/2} = \dot{m} [1.58 h_0]^{1/2} \gamma = 1.66 \quad A/A^* = 4$$

Agreement between the two values was generally better than 30% with the calculated value being higher. Therefore the thrust deflection system in the pressure range of interest can only be considered to give a relative value of the thrust to probably no better than 30% accuracy.

A second inaccuracy in the reading of the thrust measuring system occurs when it is used with the accelerator. Because of the Hall effect, the jet is deflected strongly as it is accelerated. This effect is very easy to observe and for high power operation at B field values above about 2 kgauss, the deflection of the jet is such that part of the flow misses the disk. This is also visible on the record of the thrust as a sudden change in the slope of the thrust vs magnetic field. In addition to the fact that the jet can deflect sufficiently to miss the disk, any jet deflection will serve to introduce an error by indicating a thrust value less than that measured in the direction of the jet.

B. Experimental Results

Several gases were studied in the confined duct accelerator, including hydrogen, nitrogen, and argon. Hydrogen was an obvious gas of interest for propulsion, due to its low molecular weight. The experiments with hydrogen were conducted in the duct accelerator during the time when severe erosion of materials, both electrode and insulator, was occurring; therefore, very little information was obtained regarding jet velocity after acceleration. The most important information obtained during the runs with hydrogen, was that a high operating voltage was required to maintain an arc. The maximum open-circuit voltage from the power supply for each arc was 460 v. With a hydrogen flow of 0.25 g/sec, a sustaining arc voltage of approximately 250 v was required. The voltage decreased with electrode position downstream, i.e., the highest voltage, generally above 350 v, was across the first electrode pair. During operation, the arcs were unstable and tended to be "blown out" repeatedly. The arc instability was caused partly by two factors: first, the open circuit voltage should have been higher than 460 v to obtain good stability for a 350-v arc; and second, the currents in each of the arcs were low, less than 50 amp. Arc stability generally increases with current, and experience with other gases in the accelerator has indicated that operation at 100 amp results in much greater arc stability than at 50 amp. However, power limitations did not allow operation at currents over 50 amp at high load voltage.

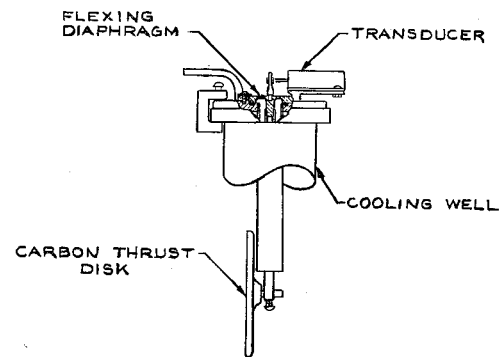


Fig. 2 Schematic of thrust measuring system.

Operation with nitrogen and argon required considerably less voltage to maintain the arc. For instance, transverse arcs in nitrogen required about 125 v with zero magnetic field, whereas in argon the voltage was about 60 v. In all cases, as the magnetic field was increased from zero, the arc voltage increased.

It is interesting to note, however, that from the point of view of efficiency, unseeded hydrogen is a poor choice as a $j \times B$ fluid. This can be seen from the fact that the increase in thrust ΔF due to the $j \times B$ force is approximately $\Delta F = BIL$, whereas the power P_E required to produce this thrust is $I \cdot V$. The ratio of thrust increment to power input is just $\Delta F/P_E = BL/V$, which says that for a given accelerator efficiency the voltage required for the arcs should be minimized. From this point of view argon should be a good possibility as a propellant.³ The forementioned, simple consideration does not account for effects such as excitation of internal degrees of freedom or de Laval expansion of the flow (with subsequent recovery of some of the power tied up in enthalpy), but it does serve as a criterion for the experimentalist. The discouraging picture as regards hydrogen as a working fluid for an efficient crossed-field propulsor may change with the addition of low ionization seed material. It should be noted, however, that a favorable propellant from the efficiency point of view, such as argon or xenon, also could be capable of high specific impulse since the accelerator action and ultimate velocity are not as dependent on sound

velocity as in the case of hot gases expanded through a de Laval nozzle.

Figure 3 shows various views of the test chamber. The magnet pole faces are $3\frac{1}{4}$ in. in height and length along the channel and are separated by $1\frac{1}{2}$ in. The magnet faces are sheathed with quartz plates $\frac{1}{4}$ -in. thick. A ridge extending $\frac{3}{16}$ in. beyond the pole faces runs along the top and bottom of each pole face: these ridges modify the fringing field of the magnet in a manner conducive to stable arc attachment. This modification can be noted on the pole face outline in Fig. 1.

Figure 3 also shows the water-cooled tungsten electrodes sheathed in boron nitride insulators as mounted during operation of the accelerator. Three electrode pairs were used during the experiments reported. The fourth pair, which was located at the entrance of the magnet channel, was unpowered and was allowed to float electrically. The three operating electrodes and their relative orientations are shown in Fig. 3. The electrode pair located furthest downstream

has the widest spacing. The tungsten rods were $\frac{1}{2}$ in. in diameter. No particular advantage was observed for any of the electrode shapes shown, and, in general, the anode showed much more erosion than the cathodes. The erosion effects on the boron nitride may be observed in the photographs. Although it is not evident from the photographs, the electrodes having square tops actually contain a hollowed cup-like depression at the tips. The other electrodes had pointed or hemispherical tips.

Figure 3 also shows the thrust disk and clearly demonstrates by the melting the effects of the transverse deflection of the plasma beam by Hall current interactions. The deflection of the jet was clearly visible through the window. The dimensions of the thrust disk and the observed erosion pattern indicate that accurate thrust measurements are not to be expected, and the recorded output of the thrust transducer represents a lower thrust than actually is being achieved. The center of the thrust disk was 2 in. from the downstream end of the accelerator and the disk was 4 in. in diameter.

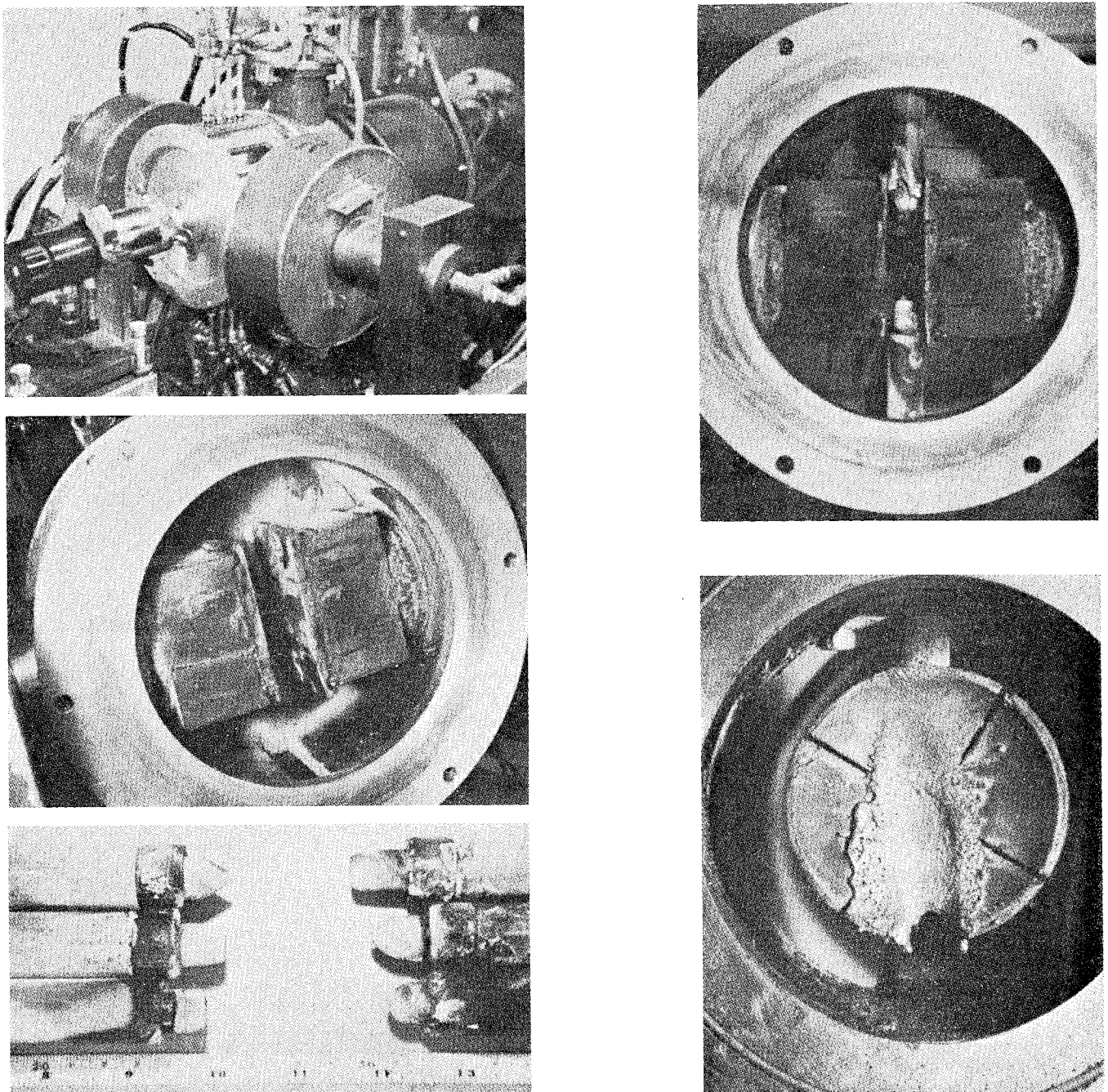


Fig. 3 Photographs of components of an open jet accelerator. The photograph in the lower right shows the melting of the thrust disk along the line of deflection of the jet.

Consequently, from simple geometric considerations, the thrust in the direction of the deflected jet, F_a , corresponding to the maximum observed thrust, F_{max} , is $F_a \approx 2^{1/2} F_{max}$. The assumption has been made that the thrust contribution due to material ejected from the face of the disk is negligible.

The variations of electrode current and voltage as functions of magnet current are shown in Fig. 4, which also shows the power consumed by each electrode. The magnetic field strength in gauss, at the center of the magnet pole gap, as a function of the magnet current, is shown in Fig. 5. Data have been plotted as a function of magnet current due to strong inhomogeneities in the field in the region of the accelerator. The curve does suffice, however, to allow approximate average values of B to be given for the accelerator. The current per electrode remains fairly constant up to fields of 1000 gauss and decreases with increasing magnetic field strength. The electrode power increases up to fields of 1000 gauss, remains fairly uniform for several hundred gauss, and

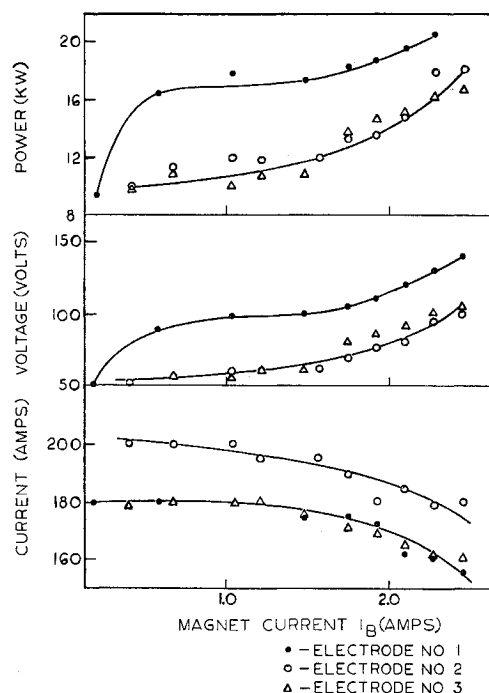


Fig. 4 Variation of the electrical parameters of the discharge for three electrode pairs as functions of the magnetic field.

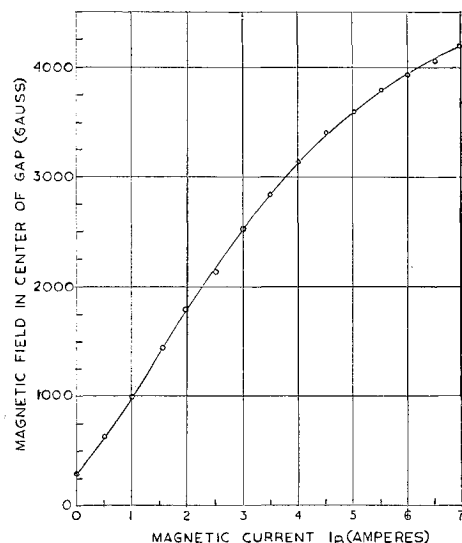


Fig. 5 Magnetic field for the gap used as a function of magnet current, I_B .

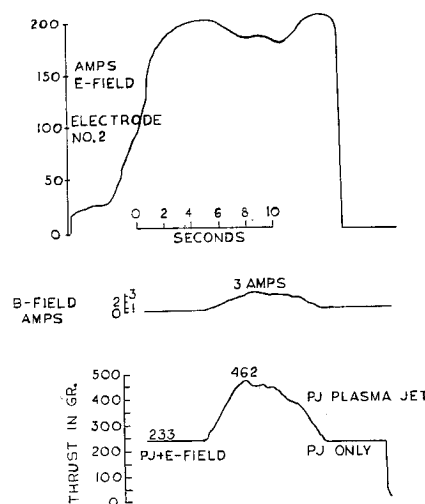


Fig. 6 Recorder tracing of a typical run.

then increases sharply. The data from which Fig. 4 was plotted were obtained with an argon flow rate of 1 g/sec and with a power input of approximately 11.6 kw to the plasma-jet "preionizer."

Figure 6 shows one portion of the recorder trace made during the same 4-min run. The thrust as a function of the product of the total electrode currents I_E and the magnet current I_B is shown in Fig. 7. The product $I_E I_B$ was chosen as the independent variable since it is proportional to $j \times B$ and is theoretically proportional to the thrust, at least according to elementary theory. The data up to $I_E I_B = 1400 \text{ amp}^2$ can be fitted to a straight line $F = 0.182 X + 228$, where F is the thrust in gram weight, uncorrected for deflections produced by Hall currents, and X is the product $I_E I_B$.

The decrease in thrust observed above $I_E I_B = 1400 \text{ amp}^2$ is attributed to the deflection of the plasma beam off the thrust disk. This is borne out by visual observation of the jet.

The average power in the E field to increase the thrust from 227 g-wt up to 400 g-wt was 40 kw. The power input to the gas, exclusive of the magnet power, was 51.6 kw for 400-g thrust. Beyond this value the E field power increased rapidly. This increase occurred in the region in which the thrust went to and beyond its maximum recorded value.

For zero field operation ($E = 0$, $B = 0$), the thrust is given approximately by $F \approx 67(\dot{m}P_H)^{1/2}$ where \dot{m} is the argon flow rate in g/sec and P_H is the power in kw to the plasma-jet. In the present case $\dot{m} = 1 \text{ g/sec}$, $P_H = 11.6 \text{ kw}$, and $F = 228 \text{ (g-wt)}$. Thus $F = 0.182 X + 67(\dot{m}P_H)^{1/2}$.

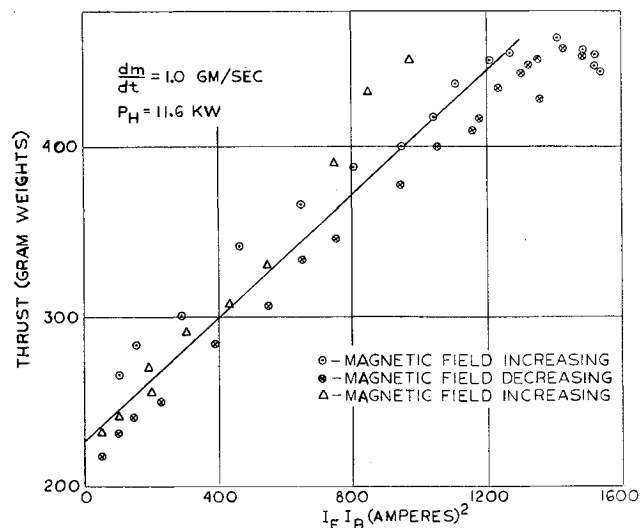


Fig. 7 The measured thrust as a function of the product of discharge and magnet current for $\dot{m} = 1.0 \text{ g/sec}$.

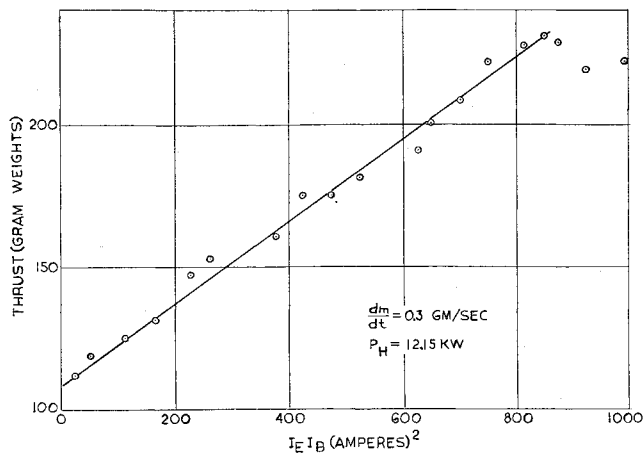


Fig. 8 The measured thrust as a function of the product of discharge and magnet current for $\dot{m} = 0.3$ g/sec.

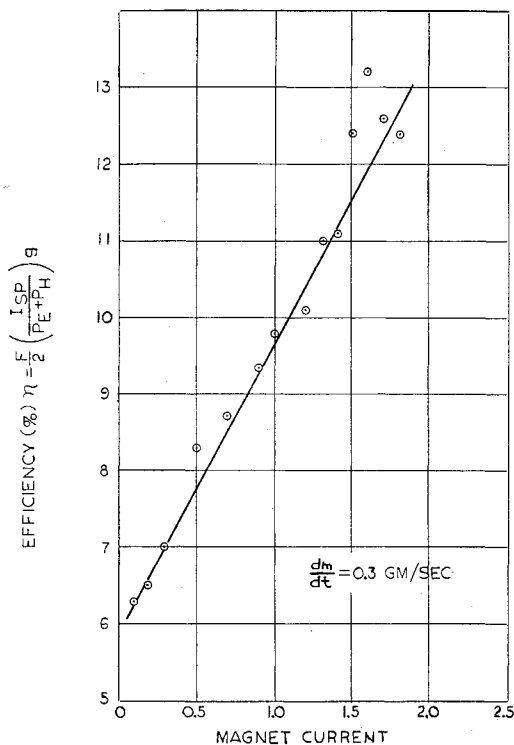


Fig. 9 Overall power efficiency as a function of magnet current.

The thrust as a function of X for a mass flow rate of 0.3 g/sec is shown in Fig. 8. In this run, $P_H = 12.15$ kw. The data can be fitted to the equation

$$F = 0.144 X + 58 (\dot{m} P_H)^{1/2}$$

The specific impulse for the 0.3 g/sec flow rate ranges from 346 sec with zero applied field to 775 sec at the highest recorded thrust. Assuming the plasma beam swept off the thrust disk at this point, as appears likely, since the thrust drops with increasing $I_E I_B$, one may estimate the "true" specific impulse (in the direction of the deflected jet) as

$$I_{sp} = 2^{1/2} I_{sp(ops)} \approx 1090 \text{ sec}$$

The power in a thrust producing plasma beam having a mean velocity v is

$$P' = vF/2 = gFI_{sp}/2$$

An efficiency η may be defined as the ratio

$$\eta = P'/(P_E + P_H) = F/2 [I_{sp}/(P_E + P_H)] g$$

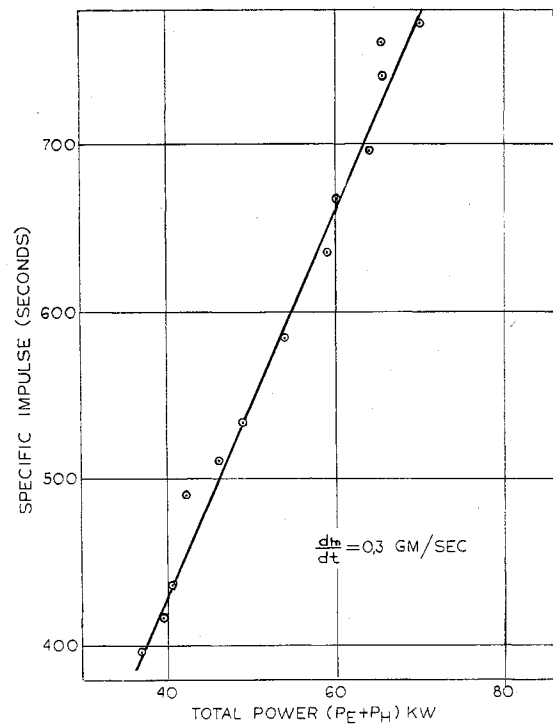


Fig. 10 Specific impulse as a function of total input power.

This efficiency has been plotted in Fig. 9 as a function of the magnet current for $\dot{m} = 0.3$ g/sec. The maximum value observed for this run was 13.2%. The efficiency should vary as $(I_{sp})^2$, i.e.,

$$\eta = \dot{m} g^2 I_{sp}^2 / 2(P_E + P_H)$$

However, the specific impulse itself is a function of the total power input, i.e.,

$$I_{sp} = h(P_E + P_H)$$

This relationship has been plotted for $\dot{m} = 0.3$ g/sec in Fig. 10. The variation is linear and the data fit the equation

$$I_{sp} \approx 10.4 (P_E + P_H)$$

where I_{sp} is in seconds and the power in kw. Once again, this represents a specific impulse derived from a thrust value that has not been corrected for the deflection of the beam. Consequently, it represents a lower limit for I_{sp} at a particular power level.

Although the present experimental work indicates the gross behavior of a continuous $j \times B$ accelerator, much more detailed study is required to acquire the information necessary to achieve useful efficiency at reasonable specific impulse and lifetime for components.

References

- ¹ Ragusa, D. and Baker, J., "Experimental results with a direct current electromagnetic accelerator," *Engineering Aspects of Magnetohydrodynamics* (Columbia University Press, New York, 1961), p. 56.
- ² Demetriades, A., "Electric-field heating threshold for charged particles," *Phys. Fluids* **5**, 1134-1136 (1962).
- ³ Hellund, E. J. and Blackman, V. H., "Crossed field accelerators," *ARS Preprint* 2128-61 (1961).
- ⁴ Kerrebrock, J. L., "Conductance in gases with elevated electron temperature," *Engineering Aspects of Magnetohydrodynamics* (Columbia University Press, New York, 1962), p. 327.
- ⁵ Demetriades, S. T., "Experimental magnetohydrodynamic engine for argon, nitrogen, and air," *Engineering Aspects of Magnetohydrodynamics* (Columbia University Press, New York, 1962).